Temporal Dynamics and Interplay of Transmission Rate, Vaccination, and Mutation in Epidemic Modeling: A Poisson Point Process Approach

Narges M. Shahtori, *Graduate Student Member, IEEE*, S. Farokh Atashzar, *Senior Member, IEEE*

***Abstract*—One of the significant challenges when a new virus circulates in a host population is to detect the outbreak as it arises in a timely fashion and implement the appropriate preventive policies to halt the spread of the disease effectively. The conventional computational epidemic models provide a state-space representation of the dynamic changes of various sub-clusters of a society based on their exposure to the virus and are primarily developed for small-size epidemics. In this work, we reformulate the conventional computational epidemic modeling approach inspired by the complex temporal dynamics observed during the COVID-19 pandemic. We utilize the Poisson point process to delineate transitions between various states, enabling us to track the exposed population effectively. The proposed model, based on random event-based Poisson arrivals, offers a comprehensive framework for understanding disease spread when the exposed state is intermediate between susceptibility and infectiousness and delays in implementing mitigation strategies are inevitable. Moreover, our newly proposed framework allows the construction of the transmission probability (p) as a probabilistic function of contributing factors such as virus mutation, immunity waning, and immunity resilience. Our results unravel the interplay between delays, transmission probability, vaccination, virus mutation, immunity loss, and their indirect impacts on the endemic states and waves of the spread. The proposed model provides a mathematical framework that allows policy-makers to improve preparedness for curtailing a lingering infectious disease spreading and unfolds the optimal time frame for vaccination given the available resources and the probability of virus mutation for the current and unforeseen outbreaks.**

***Index Terms*—Infectious disease modeling, epidemic networks modeling, Poisson point process, probabilistic epidemiological modeling, epidemiological statistical modeling**

I. Introduction

The novel coronavirus disease, also known as COVID-19, has had a major impact on the healthcare system over the last two years. Series of new cases and hospitalization spikes put intense pressure on the health care staff and resources, resulting in an estimated total loss of $323.1B and over 1 million deaths in the US alone [1].

Narges Shahtori is with the Department of Electrical and Computer Engineering, Tandon School of Engineering, New York University, New York, NY, 11201.

S. Farokh Atashzar is with the Department of Electrical and Computer Engineering and the Department of Mechanical and Aerospace Engineering. He is also affiliated with the Department of Biomedical Engineering, also with NYU WIRELESS, and NYU Center for Urban Science and Progress (CUSP). E-mail: sfa7@nyu.edu

The material presented in this work is supported by the US National Science Foundation (NSF), Award: 2208189. The work is also supported in part by Mathworks.

Some of Coronavirus's peculiar epidemiological traits and unavoidable delays in implementing the mitigation strategies make the prevention efforts to halt the spread of the disease more challenging. Particularly, epidemiological studies indicate that a significant number of carriers are asymptomatic and are unaware that they are carrying the virus [2] [3] [4].

Ongoing disease transmission and many actively infected individuals result in SARS-CoV-2 virus mutation over time, and new variants, yet more contagious, are introduced [5]. For instance, in November 2021, studies showed the $B.1.1.529$ variant, also known as omicron, which later resulted in unprecedented waves in many countries, can escape antibody immunity induced by the existing vaccines [6] [7] [8]. In addition, imperfect implementation of control strategies and failure to diagnose the symptoms of the disease or its new variants, specifically at the early stage, results in multiple surges in new cases [9], as has been observed in the last two years. This would call for more holistic modeling that matches the complex behavior of prolonged pandemic crises in a connected society, going beyond small-scale epidemic modeling [10] [11] [12].

The major challenge when a virus circulates in a host population is to detect the outbreaks as they arise in a timely fashion and implement the appropriate preventive policies. A critical question, however, is what type of management policies can be applied to effectively control the spread of infectious disease, reduce the financial burden of emerging infectious diseases on the healthcare system, and subsequently reduce the mortality rate. Contact tracing and isolation are two main strategies, the proper implementation of which can slow down the chain of virus transmission when vaccination is not immediately accessible to the mass population. However, implementation of those preventive strategies with no delays is rarely achievable, and it heavily depends on the socioeconomic status of the host population and can be a major burden for societies with limited healthcare access [9] [13]. During the coronavirus pandemic, public and private health authorities utilize different mitigation strategies such as contact tracing, isolation, and mass COVID-19 testing to curtail the outbreak. In practice, implementation of control measures in a highly connected society with no delays, detecting the most optimal strategies, large-scale optimal resource allocation, and enforcing preventive protocols within an effective timeframe when patients outnumber the health care staff and the first responders have not been feasible in most regions worldwide. Studies of other recent outbreaks, such as Ebola epidemics

in West Africa, also indicate that the spread of disease was effectively controlled once preventive protocols were improved and adequate resources were allocated to reduce the time delay in identifying and tracing newly infected individuals [14] [15].

In this regard, computational and probabilistic models that formulate the statistics of virus spread propagating among various clusters of a networked society are playing an invaluable role in providing insight into the stated problems and helping decision-makers, governments, and stakeholders to implement appropriate strategies [16] [17]. A better understanding of the impact of delays and efficacy of the conducted mitigation at different stages of disease propagation, in addition to better prediction of the effects of potential future mutations and the changes in the status of immunity resilience, are unmet needs for the control of a pandemic-level spread and can be crucial to avoid the disabling socioeconomic pressure on many societies, caused by the virus, for example, in future unforeseen outbreaks and pandemics.

Motivated by the above-mentioned facts, there has been a surge of efforts in developing various computational models in the literature. Such models provide a state-space representation of the dynamic changes of various sub-clusters of a society based on their exposure to the virus and are insightful for early-stage epidemics. For example, the commonly used method $susceptible - infected - recovered$, named SIR, models the connection and disease transmission between susceptible, infected, and recovered groups in a host population. More advanced models, such as $susceptible - exposed - infected - recovered$ ($SEIR$), include an intermediate dynamical state for the exposed group to better model the interaction between sub-populations during the course of an epidemic. Specifically, individuals in the exposed state (E) incubate the virus for a certain period of time before becoming infectious. They are considered non-symptomatic and non-infectious during this period. In some literature, additional states are incorporated into the classical $SEIR$ and SIR models to further enhance the modeling of the complex nature of disease spreading [18] [19] [20] [21] [22].

Going beyond the above-mentioned classical models, researchers tried to incorporate the mitigation strategies, immunity loss, and demographic effects into the mathematical infectious disease modeling and assess the effects on the disease transmission rate. In this regard, Radulescu *et al.* have enhanced the SEIR model by assembling an age-compartmental design and incorporating social mobility dynamics to numerically study the disease progression in a small college community scenario when social mobility restrictions are enforced [23]. In another effort, Bjørnstad *et al.* incorporate demographics and immunity loss into the classical $SEIR$ model to assess endemic states in the presence of continuous recruitment into susceptible populations [24]. However, the physics of transmission rate and average contact rate with respect to the model dynamics are disregarded in the proposed models. In a homogeneous population, we define the transmission rate (β) as $\beta = p\omega$ [25]. p is the probability of disease transmission, and an individual makes contact with the infected population (I) with the rate of ω. In reality, social mobility restrictions, mortality, and demographics directly impact the ω, p, and subsequently β and, thus, the number of new cases. The models designed in the literature often oversimplify the interdependent effects among ω, p, and model states [24] and [23]. Thus, such models often fail to take into account adequate factors that contribute to the magnitude of the epidemics, and as a result, they cannot provide the needed accuracy in the estimation of disease spread, especially at a large scale such as a pandemic.

In addition to the above, there are limited works to realistically incorporate the delays corresponding to the implementation of mitigation strategies and lack of identifiability as part of the state-space infectious disease modeling [26] [27] [9] [28]. In an effort to assess the consequences of delays and incomplete identification of infectious individuals, Young *et al.* proposed a mathematical framework that considers the average transition time from one state to another as a form of a constant delay [9]. However, the proposed model fails to capture the probabilistic nature of transition when an exposed individual incubates the virus for σ unit-time. For example, the work presented in [9] assumes that all of the susceptible individuals that come into contact with infectious individuals at time $t - \sigma$ acquire the disease at time t, and therefore, the probabilistic effect of intermediate dynamical state E (which directly impacts the spread of disease) is not observed in the model.

In this paper, to bridge the gap between the observed reality of large-scale and long-term disease progression in a host population and currently utilized infectious disease frameworks, we (1) redefine the computational representation of state transitions when the exposed individuals incubate the disease for a period of time before becoming infectious using the Poisson point process, which is characterized by its random events-based properties. Traditional state-space models neglect the possibility of exposed individuals not contracting the disease and returning to the susceptible pool. We formulate dynamic interaction behavior among various states as an arrival Poisson point process, that is, an individual in the host population arrives/departs into/from a state (given the health status) randomly within a predefined period. Specifically, this allows for tracking the exposed population and identifying those who do not contract the disease as opposed to those who become infectious and transition to the infected state. (2) Over the past three years, it has become evident that delays in implementing preventive protocols and vaccination strategies are inevitable when new diseases emerge and play a significant role in determining the behavior of a disease in its endemic state [9]. However, the existing models proposed to incorporate the delays corresponding to mitigation strategies oversimplify the probabilistic nature of the transition. In this study, we address this limitation by utilizing the Poisson framework. Here, delays are considered as another predefined period within the scope of the Poisson arrival process, allowing us to calculate the average number of arrivals to the state within these periods. By integrating this element, the model mirrors real-world scenarios where delays in response measures significantly influence disease spread. (3) Lastly, we address the often-overlooked factors of virus mutation and the

development of immunity through vaccination. Traditionally, state-space models focus on the transmission probability (p) without adequately considering how virus mutations and the evolving immunity of the population significantly alter this probability. By incorporating these dynamic factors into the model, the proposed model in this paper provides a realistic representation of disease spread for large-scale outbreaks. To this end, we introduced a novel state-space model called *Susceptible–exposed–infected–quarantine–recovered-dead* ($SEIQRD$), which considers both temporal event-based and probabilistic features of transitions across various states. Using this framework, we shed light on the critical questions pertaining to the evolution of transmission rate when control measures, such as mass vaccination, are implemented with delays.

Our simulations unravel the interplay between transmission rate, vaccination, virus mutation, and their indirect impacts on the endemic states and waves of the spread and allow for more accurate predictions and effective planning, as they mirror the actual evolving nature of the virus and the population's immune response. Additionally, to assess the performance of the proposed model with respect to COVID-19 data and infer crucial epidemiological parameters, we utilized COVID-19 data in Germany from December 11, 2020, to March 15, 2021. Our unique mathematical framework allows us to objectively evaluate and identify the optimal management policies required to effectively curtail infectious disease spread. Furthermore, our novel model provides a robust mathematical framework that allows policy-makers to improve preparedness for curtailing an infectious disease and unfolds the optimal time frame for vaccination given the available resources and the probability of virus mutation for the current and unforeseen outbreaks.

II. Overview of Mathematical Modeling

Over the years, various methods have been developed to address fundamental questions pertaining to the evolution of infectious disease in a host population and the associated risks related to reactive and proactive management policies. Computational infectious disease models allow the detection of the surge of new cases and the emergence of outbreaks at an early stage. To this end, several mathematical approaches have been introduced in the literature. Regression-based models are one of the most commonly used to predict the emergence of outbreaks. For example, one of the known models developed to estimate the average influenza mortality using the regression method is proposed by *Serfling* [29]. The model incorporates seasonal behavior, historical data on influenza, and reported cases in order to predict the emergence of new outbreaks. Over the years, major efforts have been placed to enhance *Serfling*'s model by incorporating the noise into the predictions and accounting for uncertainties [30] [31]. In another line of research related to statistical methods, researchers implement the hidden Markov model (HMM) [32] and Markov Chain Monte Carlo (MCMC) [33] to incorporate the hidden states of the disease spread and forecast the outbreak. Moreover, in recent years, the models focusing on pedestrian behavior have developed to investigate how individual actions contribute to virus transmission in broader, more complex scenarios [34] [35] [36]. Another prevalent approach for forecasting the progression of infectious disease spread utilizes state-space models. These models are instrumental in projecting the trajectory of outbreaks over time and evaluating the impact of various containment measures. Another widely used approach is the state-space model. The conventional computational epidemic models provide a state-space representation of the dynamic changes of various sub-clusters of a society based on their exposure to the virus and are primarily developed for small-size epidemics. In the next section, we reviewed this particular model.

A. State-Space Model

The conventional state-space model that allows for the incorporation of the relevant contributing factors of infectious disease spread was proposed by *Kermack and McKendrick* [37]. The state-space SIR ($susceptible - infected - recovered$) model proposed by *Kermack and McKendrick* has been widely used to predict new outbreaks and model infectious disease spread [38]. In this context, the host population is divided into different groups based on the state of their health and their interactional status with the infected sub-population. (1) represents, SIR state-space model proposed by *Kermack and McKendrick* [37].

$$\begin{aligned} \frac{dS}{dt} &= -p\omega S(t)I(t), \\ \frac{dI}{dt} &= p\omega S(t)I(t) - \gamma I(t), \\ \frac{dR}{dt} &= \gamma I(t) \end{aligned} \tag{1}$$

In the SIR model, given above, at time t, the infected sub-population, $I(t)$, makes contact with the susceptible sub-population, $S(t)$, with rate ω and a susceptible individual contract the disease with probability p. Thus, an infected person transmits the disease to $p\omega S$ susceptible individuals at a unit of time. $-p\omega SI$ term indicates the number of susceptible individuals who enter the infectious group I. Then, infected individuals move to the recovered/dead sub-population, R, within γ^{-1} unit time [39]. In this framework, the R compartment is considered the sub-population that cannot get re-infected. In addition, the size of the host population, N, is assumed to remain constant throughout the outbreak, and the host population is considered to be homogeneous, i.e., individuals in the host populations have an equal probability of making contact with others, and every susceptible individual has the same probability of becoming infected. Over the last few decades, the SIR model has been enhanced by adding another state named exposed, E. The model is also known as $susceptible - exposed - infected - recovered$ or, in short, $SEIR$. This model is widely used in the literature when exposed individuals incubate the virus for σ^{-1} unit time. (2) represents the state-space model of $SEIR$ and formulates

transitions across various states mathematically.

$$\begin{aligned}\frac{dS}{dt} &= -p\omega S(t)I(t),\\ \frac{dE}{dt} &= p\omega S(t)I(t) - \sigma E(t),\\ \frac{dI}{dt} &= \sigma E(t) - \gamma I(t),\\ \frac{dR}{dt} &= \gamma I(t)\end{aligned} \tag{2}$$

In the $SEIR$ model presented above, it is assumed that susceptible individuals leave the S group when they become in contact with infectious individuals (I) and contract the disease with a transmission probability of p. The exposed individuals (E) are considered non-symptomatic and non-infectious during the incubation period. Exposed individuals incubate the disease for σ^{-1} unit time before moving to the infectious state at rate σ. Then, infected individuals enter the recovered/dead state (R) after γ^{-1} unit time. The classic $SEIR$ model is suitable to simulate and predict early-stage of outbreaks. However, there are three major issues with the conventional $SEIR$ models concerning outlining a realistic realization of large-scale epidemics or pandemics.

- **Problem (1)** In the classic $SEIR$ model, it is assumed that individuals who contact an infectious person contract the disease with the probability of p and leave the S state with the rate of $p\omega$. However, this assumption does not take into account that a portion of the exposed population would not contract the disease and return to the S population. In reality, the interactional status between the E and the S states is directly controlled by the health authorities and policymakers for curtailing the disease spread by tracing the detected exposed individuals (also known as "contact tracing"). Recruitment of exposed individuals who do not contract the disease to susceptible sub-populations after the incubation period is an important dynamic pattern that plays an integral part in the spread of the disease and has been disregarded in the literature.
- **Problem (2)** Over the last three years and previous outbreaks, it has been shown that delays in terms of implementation of preventive protocols and vaccination are inevitable [9] [15]. The delays pertaining to mitigation strategies are another important dynamic that directly impacts the behavior of the system in the endemic state. There has been limited work to incorporate the delays corresponding to the implementation of mitigation strategies as part of the state-space infectious disease modeling, e.g., [26] [27] [9] [40] [41]. However, the proposed models oversimplify the probabilistic nature of transition and the temporal inter-dependency between p, ω, S, and I when an exposed individual incubates the virus for σ unit-time.
- **Problem (3)** Virus mutation and vaccination directly impact the probability of transmission, p, and subsequently, the number of new cases in the host populations. However, mutation and development of immunity resilience against the virus are overlooked as contributing factors in the literature when modeling the disease's spread.

In section II-B, we reviewed the Poisson point process basis, which is the foundation of our proposed model in III-A.

B. Homogeneous Poisson Point Processes

A homogeneous Poisson point process is a stochastic process that is utilized in queuing theory to model random events such as arrivals or departures in a system [42]. The Poisson point process is defined as a Poisson random variable where the Poisson parameter depends on the duration of the interval in which departure or arrival occurs. In the Poisson point process, non-overlapping intervals are considered as independent events [43] [44]. Considering these two key observations, a Poisson point process is defined as given below.

Definition II.1. Assume $X(t) = Z(t_1, t_2)$ represents a Poisson point process. The number of arrivals, k, during (t_1, t_2) interval with length of $t = t_2 \breve{} t_1$ is a Poisson random variable with parameter λt. Given that,

$$P\{Z(t_1, t_2) = k\} = e^{\lambda t}\frac{(\lambda t)^k}{k!}. \tag{3}$$

where $P\{Z(t_1, t_2) = k\}$ represents probability of having k arrival within t unit time. Considering (3), it can be mentioned that if the intervals (t_1, t_2) and (t_3, t_4) are non-overlapping, then the random variables $Z(t_1, t_2)$ and $Z(t_3, t_4)$ are independent.•

The properties of a Poisson process imply that in any interval $\delta(t)$, one event can occur with the probability that is proportional to $\delta(t)$. Furthermore, the probability that two or more events occur in the same interval is proportional to $O(\delta(t))$ [45]. The inter-arrival duration of a Poisson point process (inter-arrival duration between the $(i-1)^{th}$ and $(i)^{th}$ moments) is defined as an exponential process. The aforementioned statement is proven below.

Proof. Assume t_0 is any fixed point and $t_0 + \tau$ represents the first arrival time after t_0. Therefore, the probability of having at least one arrival within τ unit time, $F_\tau(t)$, is:

$$\begin{aligned}F_\tau(t) &= P\{\tau < t\}\\ &= P\{Z(t_0, t_0 + t) > 0\}\\ &= 1 - P\{Z(t_0, t_0 + t) = 0\} = 1 - e^{-\lambda t}\end{aligned} \tag{4}$$

We can observe that $1 - e^{-\lambda t}$ is in fact, the cumulative distribution function of the exponential distribution. Hence, we can derive the probability density function (PDF) as follows:

$$\begin{aligned}f_\tau &= \frac{dF_\tau(t)}{dt}\\ &= \lambda e^{-\lambda t}.\end{aligned} \tag{5}$$

□

Thus, considering (5), we can derive the average number of arrivals in a Poisson point process given a known interval time τ as follows [44] [46]:

$$E(f_\tau) = \frac{1}{\lambda}. \tag{6}$$

We use the Poisson point process concept presented in this section to reformulate the conventional definition of the $SEIR$ model. In section III-A, we propose a novel $SEIR$ framework by integrating the arrival Poisson point process concept into the $SEIR$ state-space model. Thus introducing a coherent

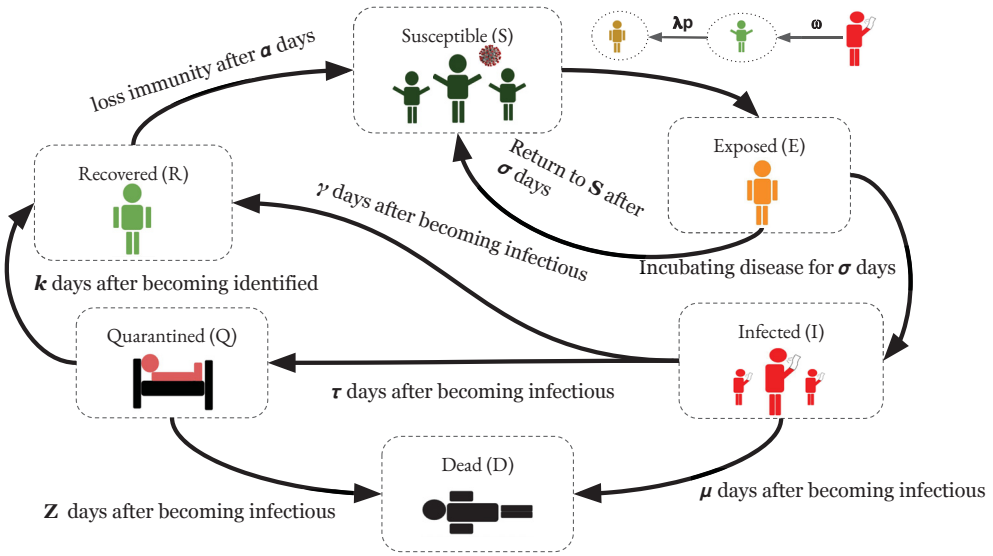

Fig. 1: A simplified summary of the proposed model ($SEIQRD$) and the corresponding spread chain: Infectious individuals become in contact with healthy individuals (S) with a rate ω. A fraction of exposed ones acquire the disease after incubating the disease for σ unit time and move to an infectious state (I) with rate $p\lambda_{EI}$. Other exposed individuals that do not contract the disease return to the susceptible population with a rate λ_{ES}. Once an exposed individual becomes infectious, they would have three possibilities: 1. they are identified and placed into isolation, state Q, 2. they recover and enter state R, or 3. they pass away (state D) and get removed from the spreading cycle. Similarly, infected individuals who are identified either recover or pass away. Finally, recovered individuals are recruited to the susceptible state due to waning immunity after α unit time with rate λ_{RS}.

Description	Parameter
Average contact rate per unit time	ω
Disease transmission rate	p
Lucky rate	λ_{ES}
Loss of immunity rate	λ_{RS}
Exposure rate	λ_{EI}
Identification rate	λ_{IQ}
The mortality rate of the unidentified infectious	λ_{ID}
The recovery rate of the unidentified infectious	λ_{IR}
The mortality rate of the identified infectious	λ_{QD}
The recovery rate of the identified infectious	λ_{QR}
Incubation period	σ
Time elapsed between recovery and loss of immunity	α
Time elapsed between infection and identification	τ
Time elapsed between identification and recovery	k
Time elapsed between identification and death	z
Time elapsed between infection and death without being identified	μ
Time elapsed between infection and recovery without being identified	γ

TABLE I: Parameters of SEIQRD model

framework that takes into account the interdependency between ω, p, and I states that are neglected in the conventional $SEIR$ model.

III. Method

In this paper, we propose a new computational model, going beyond classic $SEIR$ modeling, using a homogeneous Poisson point process for the first time that addresses the previously mentioned issues in section II-A. The proposed model in this paper, depicted in Fig. 1 and parameters delineated in Table. (I), takes into account (a) the interactional status between the E and the S states when exposed individuals do not contract the disease, (b) the inter-dependency between p, ω, S, and I states, and (c) the effects of mutation and development of immunity resilience in the society. Such a model can be imperative when controlling a long pandemic in a mega population that echoes waves of mutation and spread.

A. Reformulating $SEIR$ model

To address critical issues with the conventional $SEIR$ model, such as oversimplification of the interplay between exposed, susceptible, and infectious states, and the inter-dependency between p, ω, S, and I, we propose a novel framework for the $SEIR$ model which utilizes the Poisson point process to define transition across various states.

In a homogeneous Poisson point process, events are distributed randomly in space or time with a constant intensity, and the key assumption of independence between points implies that the occurrence of one point does not influence the probability of another point occurring within the process. In the context of our proposed model, we assume events (individual transition from one state to another) and not time are independent.

We consider the transitions between $E \rightarrow I$ and $I \rightarrow R$ as an arrival Poisson point process, meaning an individual in the host population arrives at a new state (given the health status) within a predefined period. We can model this behavior using the Poisson point process concept because the average transition period is known, but the exact arrival time to a new state is random. Specifically, Therefore, we can formulate the transition rate as the average number of arrivals (events) given the transition period using (6).

We assume a susceptible individual who becomes in contact with an infectious person leaves the susceptible group (S) with a rate ω. The newly exposed individuals, $\omega S(t)I(t)$, at time t, are considered non-symptomatic and non-infectious. Notably, only a fraction of exposed individuals become infectious. The exposed individuals who contract the disease with probability p move to the infectious state I with rate λ_{EI} after incubating the disease for σ unit time. λ_{EI} represents the average number of arrivals to state I given the transition period of σ. The exposed individuals who do not contract the disease after σ unit time, return to the susceptible population with rate λ_{ES}. Specifically, λ_{ES} represents the average number of individuals who return to state S given the transition period of σ. Then, infected individuals enter the recovered/dead state (R) with rate λ_{IR} after γ unit time. Similar to the previously introduced rates, λ_{IR} represents the average number of individuals moving to the R state given γ unit time. (7) represents the computational framework for the proposed model.

$$\begin{aligned}
\frac{dS}{dt} &= -\omega S(t)I(t) + \lambda_{ES}E(t-\sigma),\\
\frac{dE}{dt} &= \omega S(t)I(t) - p\lambda_{EI}E(t-\sigma) - \lambda_{ES}E(t-\sigma),\\
\frac{dI}{dt} &= p\lambda_{EI}E(t-\sigma) - \lambda_{IR}I(t-\gamma),\\
\frac{dR}{dt} &= \lambda_{IR}I(t-\gamma)
\end{aligned} \tag{7}$$

This framework formulates the dynamic changes of various sub-clusters of the host population based on their exposure to the virus when the exposed group is an intermediate step between the susceptible and the infectious states. The proposed model reconstructs the $S \rightarrow E \rightarrow I$ transition by considering the fact that changes in the susceptible population occur only when individuals get exposed to the virus and not when they contract the disease. Furthermore, the proposed model allows for the construction of p as a function of contributing factors. We propose a unique model for p by taking into account the relevant factors such as virus mutation, vaccination, and immunity loss in section III-B. Such a model can be utilized to simulate the future waves of pandemics depending on an assumed temporal expectation of the mutation. Also, the new formulation allows for the evaluation of the disease spread in various societies and sub-societies with different immunity responses and vaccination profiles.

B. Probabilistic temporal event-based disease progression model

To address the critical questions mentioned in section II-A and assess the impact of vaccination objectively, we proposed a novel mathematical framework that (a) takes into account the interdependent relations between transmission rate (p), contact rate (ω) and immunity loss ($\lambda_{RS}R(t-\alpha)$), and (b) formulates the dynamical temporal event-base interactional status across various states. The proposed model, *Susceptible-exposed-infected–quarantine–recovered-dead* ($SEIRQD$) divides the host population into six groups, depending on the state of an individual's health and whether or not they are exposed to the virus through an infected person.

Infectious individuals (I) become in contact with healthy individuals (S) at rate ω. A fraction of exposed ones (E) acquires the disease after incubating the disease for σ unit of time and moves to an infectious state (I) with the rate $p\lambda_{EI}$. In this paradigm, the term $\omega S(t)I(t)$ represents the number of individuals who become in contact with infected individuals at time t. A fraction of those who are exposed to the virus at time $t-\sigma$ (i.e., $E(t-\sigma)$) contract the disease after incubating the virus for a period of σ unit time. During this period, they are considered non-symptomatic and non-infectious. Once an exposed individual becomes infectious, they would have 3 possibilities: (1) they are identified and placed into isolation, state Q, (2) they recover and enter state R, or (3) they pass away (state D) and get removed from the spreading cycle. The exposed individuals who do not contract the disease after σ unit time return to the susceptible population with rate λ_{ES}. Infected individuals who are identified either recover or pass away. Finally, recovered individuals are recruited to the susceptible state after α unit time with rate λ_{RS}.

$$\begin{aligned}
\frac{dS}{dt} &= -\omega S(t)I(t) + \lambda_{RS}R(t-\alpha) + \lambda_{ES}E(t-\sigma),\\
\frac{dE}{dt} &= \omega S(t)I(t) - p\lambda_{EI}E(t-\sigma) - \lambda_{ES}E(t-\sigma),\\
\frac{dI}{dt} &= p\lambda_{EI}E(t-\sigma) - \lambda_{IR}I(t-\gamma)\\
&\quad - \lambda_{IQ}I(t-\tau) - \lambda_{ID}I(t-\mu),\\
\frac{dQ}{dt} &= \lambda_{IQ}I(t-\tau) - \lambda_{QR}Q(t-k) - \lambda_{QD}Q(t-z)\\
\frac{dR}{dt} &= \lambda_{IR}I(t-\gamma) + \lambda_{QR}Q(t-k) - \lambda_{RS}R(t-\alpha)\\
\frac{dD}{dt} &= \lambda_{QD}Q(t-z) + \lambda_{ID}I(t-\mu)
\end{aligned} \tag{8}$$

(8) represents the proposed $SEIQRD$ mathematical model. Individuals move to a new group (e.g. arrive in a new group) after staying in the current group for y unit time. We formulate this behavior using the homogeneous Poisson process because the average transition time is known, but the exact arrival time to the new state is random. Per (5) and (6), the average inter-arrival duration between $i-1^{th}$ and i^{th} moments in a Poisson point process with rate λ forms an exponential distribution,

with the expected value of λ^{-1}. Therefore, we define the $E \rightarrow I$, $E \rightarrow S$, $I \rightarrow D$, $I \rightarrow Q$, $I \rightarrow R$, $Q \rightarrow R$, $Q \rightarrow D$ transitions as follows:

- $E \rightarrow I$: During σ unit time, on average λ_{EI}^{-1} exposed individuals who contracted the virus with probability p undergo a transition to state E. This implies that exposed individuals who become infectious enter state I with σ unit time delay with the average rate of λ_{EI} which is reflected as $p\lambda_{EI}E(t-\sigma)$ in (8).
- $E \rightarrow S$: During σ unit time, on average λ_{ES}^{-1} exposed individuals that do not contract the virus undergo a transition to state S. This implies that exposed individuals who are not infectious return to state S with σ unit time delay with the average rate of λ_{ES} which is reflected as $\lambda_{ES}E(t-\sigma)$ in (8).
- $I \rightarrow D$: The infected individuals at time $t-\mu$ pass away with the average rate of λ_{ID} after remaining contagious for μ unit time. Particularly, the arrival at state D between the $(i-1)^{th}$ and $(i)^{th}$ moments is an exponential random variable with rate λ_{ID}^{-1}. This transition is indicated in (8) as $\lambda_{ID}I(t-\mu)$.
- $I \rightarrow Q$: The average number of infectious who are identified during τ unit time is λ_{IQ}^{-1}. Therefore, the infectious individuals at time $t-\tau$ undergo a transition to state Q with the average rate of λ_{IQ} at time t. This behavior is modeled as $\lambda_{IQ}I(t-\tau)$ in (8).
- $I \rightarrow R$: During γ unit time, the average number of unidentified infected individuals who are recovered is λ_{IR}^{-1}. As a result, infectious individuals at time $t-\gamma$ move to state R with the average rate of λ_{IR} at time t. This behavior is modeled as $\lambda_{IR}I(t-\gamma)$ in (8).
- $Q \rightarrow R$: Term $\lambda_{QR}Q(t-k)$ in (8) indicates the number of identified infected individuals at time $t-k$ who are recovered with the average rate of λ_{QR} at time t.
- $Q \rightarrow D$: Term $\lambda_{QD}Q(t-z)$ defines the changes in quarantine population at time t. These individuals enter group Q at time $t-z$ and pass away at the average rate of λ_{QD}.
- $R \rightarrow S$: Individuals who are recovered at time $t-\alpha$ maintain immunity against the disease for α unit time and immunity wanes with the average rate of λ_{RS}.

The proposed model in this section maps out the interplay between various states by taking into account the complex temporal interaction and inherent dynamics. However, to assess the impact of vaccination on the transmission rate and, ultimately, the disease propagation, we need to define p as a function of relevant factors, i.e., virus mutation, vaccination, and immunity loss. In the next section, we propose a framework that can be integrated with the proposed model to represent the response of the system to mutation, vaccination, and immunity loss. Such a model can be utilized to simulate the future waves of pandemics depending on an assumed temporal expectation of the mutation. Also, this allows for the evaluation of the disease spread in various societies and subsocieties with different immunity responses and vaccination profiles.

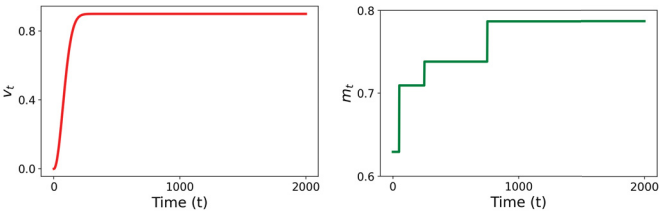

(a) (b)

Fig. 2: (a) The simulated realization for vaccination function, $v(t)$ represents the host population's immunity against the virus. (b) Simulated realization of mutation function, $m(t)$. (10) is utilized with parameters $\eta_1 = 9e{-}1$ and $\eta_2 = 1e{-}4$ to generate $v(t)$ function. (11) is utilized to generate a realization of virus mutation, $m(t)$, due to ongoing disease transmission results.

C. Disease transmission rate

We formulate $p(t)$ by incorporating virus mutation, waning immunity, and the population's immunity resilience against the virus as given below:

$$\frac{dp}{dt} = -[\delta + \zeta_0 v(t)]\zeta_1 p(t) + \zeta_2 m(t) \tag{9}$$

(9) represents the mathematical expression of $p(t)$. In this model, $v(t)$ reflects the host population's immunity resilience against the virus boosted by vaccination efforts, and $m(t)$ indicates the communication of virus variants from one person to another. ζ_1 represents the overall rate at which immunity is produced against the virus in the host population through vaccination and natural immunity. ζ_0 represents how well the vaccination efforts are implemented. ζ_2 is the rate at which the virus spreads given the circulating variant at time t. Infected individuals who recovered develop natural immunity against the virus, which results in a reduction of $p(t)$ over time. We formulate this behavior by adding $-\zeta_1\delta p(t)$ term in (9). We use (10) to generate a sigmoid shape curve for $v(t)$. Particularly, this function generates an *S-shape* growth curve in which immunity resilience boosted by vaccination increases slowly initially and approaches an exponential growth rate when mass vaccination becomes available.

$$v(t) = \eta_1(1 - e^{-\eta_2 t^l}) \tag{10}$$

The virus variant's contagion rate is modeled using (11). We utilize multi-step functions as indicated in (11) to take into account virus mutation occurrence and model the corresponding contagion rate.

$$\begin{aligned} m(t) &= \sum_{i=1}^{n} \Delta_i \Phi_i(t) \\ \Phi_i(t) &= c_i, \quad t \in [t_{i-1}, t_i], \end{aligned} \tag{11}$$

IV. Simulation Results

In this subsection, we systematically examine the potential outcomes of the proposed model given by (8). Specifically, we explore scenarios when resources permit vaccinating 80% of the host population across different average contact situations.

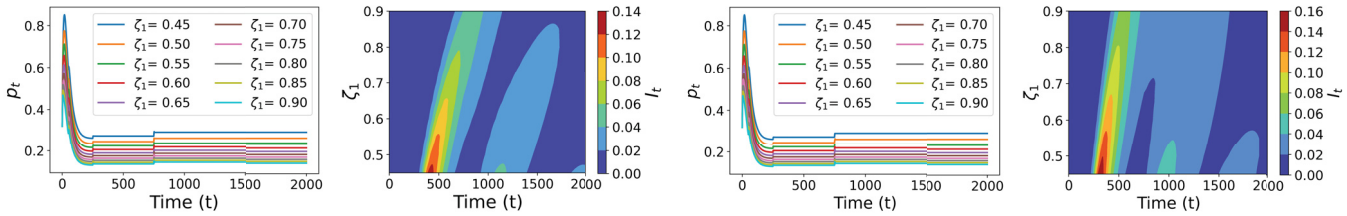

(a) (b)

Fig. 3: (a) Simulated realization for transmission rate, $p(t)$ when average contact rate, $\omega = 0.5$ and (b) when $\omega = 0.7$. It represents the evolution of $p(t)$ over time with respect to virus mutation, the performance of vaccination implementation, and natural immunity built-up. ζ_1 plays an input control role, which defines how effective mass vaccination efforts are implemented in the host population.

We explore a comprehensive simulation study to understand the dynamics of the proposed model as defined by (8) and (9). Our objective is to generate realistic projections of infectious disease spread and assess the influence of large-scale vaccination in mitigating the spread. For our simulations, we set the population size as $N = 8 \times 10^6$, starting with $I_0 = 1$ infected individuals. At the onset, $t = 0$, the transmission rate is designated as $p(0) = 0.32$. The study envelops average contact rates, ω, within the range $[0.5, 0.7]$. Given the virulent nature of the ailment, we have assigned an elevated exposure rate of $\lambda_{EI} = 0.036$, coinciding with an incubation span of $\sigma = 5$ time units. This configuration implies that an average of 27 individuals, upon exposure at rate p, progress to the infectious phase within σ time units. Post incubation, exposed individuals not contracting the disease transition back to the susceptible bracket at a rate of $\lambda_{ES} = 0.034$. Infected cohorts subsequently:

- Recover, governed by a rate of $\lambda_{IR} = 0.014$, within a time frame of $\gamma = 14$ units.
- Or, pass away at a rate of $\lambda_{ID} = 0.0008$, within $\mu = 15$ time units.
- A subset undergoes identification at a rate of $\lambda_{IQ} = 0.0152$, in a span of $\tau = 5$ time units. These diagnosed individuals are quarantined, curtailing any further exposure. Their isolation persists for $k = 21$ time units, post which they either integrate into the R state at a rate of $\lambda_{QR} = 0.0008$, or pass away after $z = 25$ time units at a rate of $\lambda_Q D = 0.00056$.

After an immunity period of $\alpha = 200$ time units, recovered individuals are reinstated to the susceptible pool at a rate of $\lambda_{RS} = 0.0032$. We employed (9) to model the time-dependent transmission rate, incorporating three virus mutations within the initial 750 time units. These variants emerged at $t = [50, 250, 750]$, with their contagion rates depicted in Fig. 2b. The contagion rate, formulated using (11), is given by:

$$m(t) = \begin{cases} 0.629, & t < 50, \\ 0.709, & 50 \leq t < 250, \\ 0.739, & 250 \leq t < 750, \\ 0.787, & t \geq 750, \end{cases} \tag{12}$$

To quantitatively gauge vaccination's role in $p(t)$ and disease control, we focused on ζ_1 as a controlling parameter. Per (9), $p(t)$'s determinants are ζ_0, ζ_1, and ζ_2. While ζ_2 is inherent, defined by the virus variant, ζ_0 and ζ_1 offer external control avenues. Fig. 2a displays vaccination coverage over 2000 time units. Parameters were set to $l = 2$, $\eta_1 = 0.9$, and $\eta_2 = 0.0001$ to simulate a feasible 80% population vaccination within the timeframe. We assigned post-recovery impact as $\zeta_0 = 1$ and inherent viral virus contagion rate as $\zeta_2 = 0.2$. Natural immunity, δ, post-recovery, is postulated at $\delta = 0.3$. To evaluate vaccination efficiency, we executed ten scenarios varying ζ_3 within the specified range delineated in 13

$$\zeta_3 = 0.45 + 0.05n, \quad n \in \{0, 1, 2, \ldots, 9\} \tag{13}$$

Fig. 3a and Fig. 3b illustrate the evolution of p when $\zeta_1 \in \{0.45 + x \leq 0.9, x = .05\}$ and $\omega \in [0.5, 0.7]$. During the first 250 unit time, p reaches its maximum value ~ 0.9 due to multiple virus mutations (Fig. 2b) and insufficient immunity resilience against virus represented in (9). However, p reduces when the host population's immunity resilience increases and eventually converges. As shown in Fig. 4a and Fig. 4b, the most significant jump in the number of new cases occurs when $p(t)$ reaches its maximum value ~ 0.9 for both $\omega = 0.5$ and $\omega = 0.7$, which indicates the direct relationship between the number of cases (I_t) and p_t. When $p(t) > 0$, the disease persists within the host community, as exemplified in Fig. 3a and Fig. 3b. The magnitudes of $p(t)$ and ω emerge as decisive factors influencing the size of the infectious cohort. In Fig. 4, the complex interplay among the model's six states and p_t is delineated. Notably, the recovered demographic displays non-linear growth patterns. These oscillations become more pronounced for diminished ζ_1 values, highlighting the challenges of limited immunity resilience, especially against various virus iterations. Two key elements accentuate the transition to the infectious state: (1) transient immunity duration and (2) ensuing immunity attrition. A robust immunity resilience can channel the host populace towards two potential trajectories:

1) A decline in the epidemic due to a contraction in infectious instances.
2) A moderated transference of exposed individuals to infectious states, courtesy of the shield offered by sturdy immunity.

We analyzed the temporal progression of I in relation to S as depicted in Fig. 5b and Fig. 5a. Observably, for $p(t) > 0$,

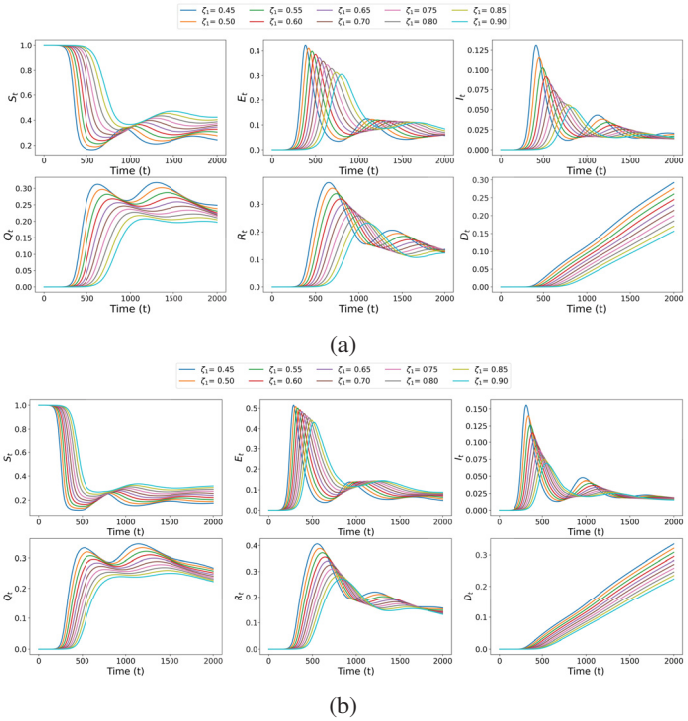

(a)

(b)

Fig. 4: (a) Simulated realization of $SEIQRD$ (8) model's states when $\omega = 0.5$ and $\zeta_1 \in \{x + 0.45 \leq 0.9\}$ (b) when $\omega = 0.7$ and $\zeta_1 \in \{x + 0.45 \leq 0.9\}$. 4a and 4b represents the evolution for infectious (I), susceptible (S), exposed (E), recovered (R), quarantined (Q) and dead states (D) in 2000 unit time span. Our simulation shows that the disease spreading continues when the transmission rate $p > 0$ (3b and 3a).

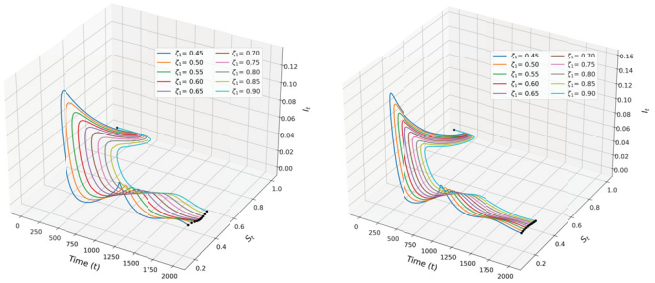

(a) (b)

Fig. 5: (a) Trajectory of dynamical states infectious (I) and susceptible (S) states over time when average contact rate is $\omega = 0.5$. (b) when $\omega = 0.7$. In this view, when the transmission rate, $p(t) > 0$, the trajectories move outwards and diverge away, which indicates an open epidemic state, meaning at any given time t, the communicable disease circulates in a sub-cluster of the host population. In addition, a series of new cases and spikes are unavoidable due to waning immunity and recruitment to the susceptible population.

trajectories diverge, signifying an active epidemic phase. This suggests that the disease remains prevalent within specific subgroups of the host population, which aligns with our results in Fig. 3a and Fig. 3b. Due to diminishing immunity and a replenishing susceptible pool, recurrent surges in cases are inherent. Our findings highlight the interplay of transmission rate, contact frequency, and immunity duration in determining disease spread and underscore the nuanced balance between transmission rate, contact propensity, and immunity resilience in steering the course of infectious dynamics.

V. Experimental Results and Discussions

In this section, to validate the efficacy of our model concerning real-world COVID-19 data and extract key epidemiological parameters, we use COVID-19 data from Germany, spanning December 11, 2020, to March 15, 2021. We utilized the extensive dataset provided by Johns Hopkins University's COVID-19 repository [47] as a cornerstone for our analysis. The rich and real-time nature of this dataset allowed us to calibrate and validate our computational model accurately. We specifically target the timeframe spanning from December 11, 2020, to March 15, 2021, a pivotal juncture within the COVID-19 pandemic timeline in Germany, which contains 96 distinctive data points. We have selected this timeframe to rigorously evaluate the effectiveness of the proposed $SEIRQD$ model, as it uniquely aligns with the convergence of two pivotal factors, underscoring the model's novelty and its relevance within this study. December 25, 2020, marked the commencement of the COVID-19 vaccination campaign in Germany. Additionally, this timeframe encapsulates the emergence of two notable virus mutations with significant implications for disease transmission. The first mutation, the $B.1.617.2$ variant (commonly known as the delta variant), was initially identified in India and began circulating around December 15, 2020, in Germany. Subsequently, on February 25, 2021, the $BA.2.86$ variant, initially originating in Britain, emerged as another prominent strain [48].

We conduct an analysis using the proposed model (8) against the COVID-19 data in Germany during the aforementioned timeframe. We integrated mutation and vaccination dynamics into epidemiological differential equations using (9). We examine three distinct scenarios: 1) including vaccination and mutations, 2) including mutations and excluding vaccination, and 3) excluding both vaccination and mutations. The primary objective of these scenarios is to evaluate the influence of vaccination while simultaneously comparing the model's performance when either mutation or vaccination dynamics are excluded. To assess the overall impact of vaccination interventions on the spread of COVID-19 in Germany during this timeframe, we examined the initial phase of vaccine implementation, which collided with existing mitigation measures, such as lockdowns. We maintain a constant average contact rate as $\omega = 0.3$ during this phase. Our population size, represented as N, is considered to be 83 million [49], and the influence of natural births and deaths is considered negligible compared to the size of the host population. For our temporal calculations, we use the unit-time measurement of one day.

We assume the incubation period is $\sigma = 8$ days [50] with transition rate of $\lambda_{EI} = 1.19e{-}2$ and $\lambda_{ES} = 5e{-}2$.

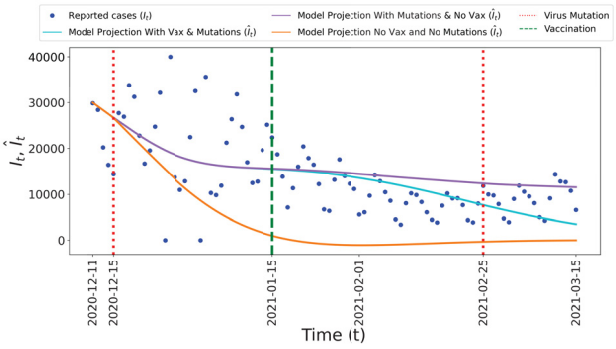

(a)

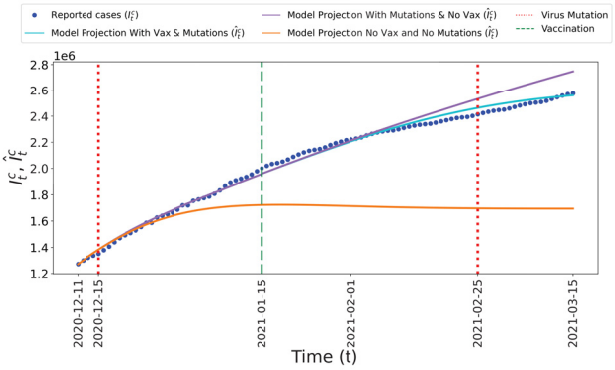

(b)

Fig. 6: (a) $SEIRQD$ model projection for daily infected cases ($\hat{I}_t$) vs reported cases in Germany (I_t) (b) $SEIRQD$ model projection for cumulative infected cases ($\hat{I}_t^c$) vs reported cumulative cases in Germany (I_t^c).

Infected individuals get identified after $\tau = 10$ with rate $\lambda_{IQ} = 1.04e{-}2$, pass away without identification after $\mu = 25$ days with rate $\lambda_{ID} = 7.9e{-}4$ or recover without identification with transition rate of $\lambda_{IR} = 2.6e{-}2$ after $\gamma = 14$ days [51]. Infected individuals that are identified pass away after $z = 25$ with rate $\lambda_{QD} = 5.6e{-}4$ or recover with rate $\lambda_{QR} = 1.8e{-}3$ within average period of $k = 20$ days. Lastly, we assume recovered individuals get recruited to state S after $\alpha = 120$ with a transition rate of $\lambda_{RS}S = 7.2e{-}3$.To estimate the initial conditions, we utilized data from the Johns Hopkins dataset starting from the previous date, e.g., December 10, 2020 and assumed $E_t^{init} = 60000$, $I_t^{init} = 30000$, $Q_t^{init} = 15000$, $R_t^{init} = 19000$, $D_t^{init} = 24000$, $p_t init = 0.42$ and $S_t^{init} = N - E_t^{init} - I_t^{init} - Q_t^{init} - R_t^{init} - D_t^{init}$. We set $l = 5$, $\eta_1 = 9e{-}1$ and $\eta_2 = 1e{-}10$ in (10) to generate a realization of the number of vaccinated individuals by *April 2021* according to the available data.

By *April 2021*, available resources allowed the policymakers to provide the first dose of vaccination for roughly 40% [47] of the German population (v_t). To generate a realization of transmission rate with respect to vaccination efforts and mutation, we use (9). We set $\zeta_0 = 4$, $\zeta_1 = 6e{-}1$ and $\zeta_2 = 2e{-}1$ in (9). We also assume that the natural immunity factor is $\delta = 3e{-}1$. We formulated the contagion rate using (11) as follows:

$$m(t) = \begin{cases} 0.56, & t < 2020/01/15, \\ 0.64, & 2020/01/15 \leq t < 2021/02/25, \\ 0.69, & t \geq 2021/02/25, \end{cases} \quad (14)$$

Fig. 6 illustrates model projection for daily cases (6a) and cumulative case (6b) in three scenarios in comparison to the reported cases. Fig. 6 illustrates when both vaccination and mutation dynamics are incorporated into the model. It yields projections that closely track the reported cases, both on a daily and cumulative basis. This alignment between the model's predictions and actual data underscores the model's ability to capture the complex interplay of factors that influenced the pandemic's trajectory during the specified timeframe. Furthermore, the model exhibited noticeable shortcomings when excluding vaccination or mutation dynamics. Specifically, in scenarios where vaccination is excluded, the model consistently overestimated the reported cases, highlighting the critical role of vaccination in curbing the spread of the virus. Conversely, when mutations and vaccination are excluded, the model demonstrates an underperformance, emphasizing the significance of accounting for the evolving viral variants and implementation of vaccination. In Fig. 7, we visually represent the model's evolutionary stages, specifically focusing on the roles of mutations and vaccination. When we exclude both vaccination and mutation from the model, an increase in the transition of individuals from the recovered (R) state to the susceptible (S) state is observed. However, the parameter p does not experience a significant increase in this scenario when compared to others. In scenarios (1) and (2), we observe a gradual increase in the parameter p_t, starting from 3×10^{-4} and reaching 3.2×10^{-4}. When vaccination is included as a contributing factor in the scenario (1), we notice a gradual rise in the recruitment of individuals into the S population from the exposed population (E) upon the introduction of vaccination. Interestingly, despite this increase in susceptibility, the number of infected individuals does not see a significant rise when compared to the scenario where vaccination is excluded, but the mutation is included (scenario (2)), while the parameter p remains within the same range for both scenarios. This suggests that vaccination has a significant impact on the dynamics of the model, transiting from state E to S, influencing the recruitment of susceptible individuals without causing a substantial surge in infections when mutations are taken into account. This trend is consistent with our earlier findings in Section III-B, where we discussed how the resilience of immunity plays a crucial role in determining the rate at which exposed individuals transition to infectious states. To accurately measure the discrepancy between predicted and actual data in real-world scenarios across three distinct settings, we used the Mean Squared Error (MSE) and Normalized Mean Squared Error (NMSE) as our primary metrics, with a specific focus on the daily new case predictions. In scenario (1), the MSE was 6.830×10^{-9}, representing the average squared difference between the model's predictions and the observed data. The NMSE, which was 0.029, normalizes the MSE by the squared range of the true values (the difference between

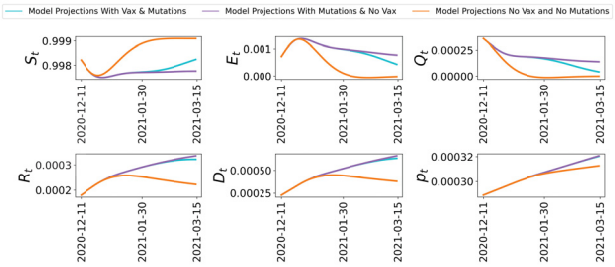

Fig. 7: States (S_t, E_T, R_t, Q_t and R_t) and p_t projections with respect to the fitted model, virus mutations, and implemented vaccination efforts.

the maximum and minimum reported new cases), enabling comparison across different scenarios. In scenario (2), both the MSE and NMSE increased, reaching 2.171×10^{-8} and 0.094, respectively. This elevation suggests a decrease in prediction accuracy compared to scenario (1). In scenario (3), while the MSE was 7.394×10^{-9}, the NMSE stood at 0.032, indicating lower accuracy relative to scenario (1). In summary, our framework is crafted to explore scenarios involving large-scale endemics, taking into direct account crucial contributing factors such as vaccination and mutations as input controls. The simulation and experimental results examined the potential influence of vaccination. In the simulation section, we evaluated the system behavior when resources permit the inoculation of 80% of the host population. Additionally, in the experimental section, we evaluated the effectiveness of our proposed Poisson point process model across different states as described in equation (8) and probability transmission rate formulations proposed in (9) with reference to COVID-19 data from Germany during a pivotal timeframe.

This paper introduces a new computational model utilizing a homogeneous Poisson point process, addressing critical limitations in conventional state-space infectious disease modeling. The recruitment of exposed individuals who do not contract the disease back into susceptible sub-populations after the incubation period is often overlooked in the literature but crucial dynamic pattern. Our proposed model tackles this issue by redefining probabilistic transitions among different states, including the $S \rightarrow E \rightarrow I$ progression, through the use of an event-based Poisson arrival process. In the Poisson point process, individuals within the host population enter or exit states randomly within predefined time intervals. While the average transition period is known in disease spread modeling, the exact timing of state transitions is random. Therefore, the transition rate between various states is formulated as the average number of arrivals (events) within the transition period. Moreover, the Poisson framework facilitates the incorporation of delays linked with mitigation strategies, significantly influencing the system's behavior in an endemic state. There has been limited work to incorporate the delays corresponding to the implementation of mitigation strategies as part of the state-space infectious disease modeling [52] [9]. However, the proposed models oversimplify the probabilistic nature of transition. Specifically, our model treats delays as additional predefined periods in the scope of the Poisson arrival process and calculates the average number of arrivals to the state within these periods. Lastly, virus mutation and vaccination directly impact the p and, subsequently, the number of new cases in the host populations. However, mutation and development of immunity resilience against the virus are overlooked as contributing factors in the literature when modeling the disease's spread. our proposed model considers mutation, development of immunity resilience, and immunity loss as part of the state-space model. This framework enables the assessment of disease spread across diverse societies and sub-societies, considering mitigation implementation delays, immunity responses, and vaccination profiles. Our model offers a robust framework crucial for managing prolonged pandemics in large populations affected by waves of mutation and implementation delays. Additionally, it simulates future pandemic waves based on anticipated timelines for mitigation strategies and mutation occurrences. Our model provides a mathematical foundation empowering policymakers to enhance preparedness and determine optimal vaccination timing given available resources for current and potential outbreaks. By utilizing our framework, health authorities gain a powerful and adaptable tool to objectively conceptualize and forecast the endemic state, considering mitigation interventions and vaccination deployment.

VI. Future Research

Future direction of research includes expanding the model to incorporate additional complexities such as spatial heterogeneity in a large multi-clustered society, demographic factors, and behavioral dynamics, including mobility in a networked model designed based on the proposed framework. This can further enhance the translational impact for complex future pandemic modeling at a large scale. Furthermore, exploring optimization techniques based on the proposed model for resource allocation in terms of mitigation strategies and vaccination would offer practical suggestions for public health decision-makers.

VII. Acknowledgement

The material presented in this work is supported by the US National Science Foundation (NSF), Award: 2208189. The work is also supported in part by Mathworks.

References

[1] A. H. Association *et al.*, "Hospitals and health systems continue to face unprecedented financial challenges due to covid-19," *Published June*, 2020.

[2] L. Luo, D. Liu, X.-l. Liao, X.-b. Wu, Q.-l. Jing, J.-z. Zheng, F.-h. Liu, S.-g. Yang, B. Bi, Z.-h. Li *et al.*, "Modes of contact and risk of transmission in covid-19 among close contacts," *MedRxiv*, 2020.

[3] S. Asadi, N. Bouvier, A. S. Wexler, and W. D. Ristenpart, "The coronavirus pandemic and aerosols: Does covid-19 transmit via expiratory particles?" pp. 635–638, 2020.

[4] T. K. Chan, "Universal masking for covid-19: evidence, ethics and recommendations," *BMJ Global Health*, vol. 5, no. 5, p. e002819, 2020.

[5] J. Chen, R. Wang, N. B. Gilby, and G.-W. Wei, "Omicron (b. 1.1. 529): Infectivity, vaccine breakthrough, and antibody resistance," *ArXiv*, 2021.

[6] N. L. Miller, T. Clark, R. Raman, and R. Sasisekharan, "Insights on the mutational landscape of the sars-cov-2 omicron variant," *bioRxiv*, 2021.

[7] S. Collie, J. Champion, H. Moultrie, L.-G. Bekker, and G. Gray, "Effectiveness of bnt162b2 vaccine against omicron variant in south africa," *New England Journal of Medicine*, 2021.

[8] W. F. Garcia-Beltran, K. J. S. Denis, A. Hoelzemer, E. C. Lam, A. D. Nitido, M. L. Sheehan, C. Berrios, O. Ofoman, C. C. Chang, B. M. Hauser *et al.*, "mrna-based covid-19 vaccine boosters induce neutralizing immunity against sars-cov-2 omicron variant," *Cell*, 2021.

[9] L.-S. Young, S. Ruschel, S. Yanchuk, and T. Pereira, "Consequences of delays and imperfect implementation of isolation in epidemic control," *Scientific reports*, vol. 9, no. 1, pp. 1–9, 2019.

[10] Y.-C. Chen, P.-E. Lu, C.-S. Chang, and T.-H. Liu, "A time-dependent sir model for covid-19 with undetectable infected persons," *IEEE Transactions on Network Science and Engineering*, vol. 7, no. 4, pp. 3279–3294, 2020.

[11] H. Kang, M. Sun, Y. Yu, X. Fu, and B. Bao, "Spreading dynamics of an seir model with delay on scale-free networks," *IEEE Transactions on Network Science and Engineering*, vol. 7, no. 1, pp. 489–496, 2020.

[12] B. Prasse and P. Van Mieghem, "Network reconstruction and prediction of epidemic outbreaks for general group-based compartmental epidemic models," *IEEE Transactions on Network Science and Engineering*, vol. 7, no. 4, pp. 2755–2764, 2020.

[13] A. James, M. J. Plank, R. N. Binny, A. Lustig, N. Steyn, S. Hendy, A. Nesdale, and A. Verrall, "Successful contact tracing systems for covid-19 rely on effective quarantine and isolation," *medRxiv*, 2020.

[14] M. J. Ryan, T. Giles-Vernick, and J. E. Graham, "Technologies of trust in epidemic response: openness, reflexivity and accountability during the 2014–2016 ebola outbreak in west africa," *BMJ Global Health*, vol. 4, no. 1, p. e001272, 2019.

[15] W. E. R. Team, "Ebola virus disease in west africa—the first 9 months of the epidemic and forward projections," *New England Journal of Medicine*, vol. 371, no. 16, pp. 1481–1495, 2014.

[16] D. Vrabac, M. Shang, B. Butler, J. Pham, R. Stern, and P. E. Paré, "Capturing the effects of transportation on the spread of covid-19 with a multi-networked seir model," *IEEE Control Systems Letters*, vol. 6, pp. 103–108, 2022.

[17] C. Ma, X. Li, Z. Zhao, F. Liu, K. Zhang, A. Wu, and X. Nie, "Understanding dynamics of pandemic models to support predictions of covid-19 transmission: Parameter sensitivity analysis of sir-type models," *IEEE Journal of Biomedical and Health Informatics*, vol. 26, no. 6, pp. 2458–2468, 2022.

[18] L. Kalachev, E. L. Landguth, and J. Graham, "Revisiting classical sir modelling in light of the covid-19 pandemic," *Infectious Disease Modelling*, vol. 8, no. 1, pp. 72–83, 2023.

[19] A. Sebbagh, C. E. Bencheriet, and S. Kechida, "A stochastic epidemiological sird-v model with lsm-ekf algorithm for forecasting and monitoring the spread of covid-19 pandemic: Real data," *IEEE Access*, 2024.

[20] L. Li, G. Liu, Q. Yu, C. Luo, X. Li, and N. Li, "Adaptive propagation model of network hotspot events based on seir," in *2023 3rd International Symposium on Computer Technology and Information Science (ISCTIS)*. IEEE, 2023, pp. 604–608.

[21] X. Li, X. L. He, M. Pu, and R. Xiao, "Prediction of epidemic transmission index based on adjusted_seir and lstm network model," in *2023 IEEE 6th International Conference on Pattern Recognition and Artificial Intelligence (PRAI)*. IEEE, 2023, pp. 1110–1117.

[22] R. Li, C. J. E. Metcalf, N. C. Stenseth, and O. N. Bjørnstad, "A general model for the demographic signatures of the transition from pandemic emergence to endemicity," *Science Advances*, vol. 7, no. 33, p. eabf9040, 2021.

[23] A. Rădulescu, C. Williams, and K. Cavanagh, "Management strategies in a seir-type model of covid 19 community spread," *Scientific reports*, vol. 10, no. 1, pp. 1–16, 2020.

[24] O. N. Bjørnstad, K. Shea, M. Krzywinski, and N. Altman, "The seirs model for infectious disease dynamics." *Nature Methods*, vol. 17, no. 6, pp. 557–559, 2020.

[25] J. R. Rohr, C. B. Barrett, D. J. Civitello, M. E. Craft, B. Delius, G. A. DeLeo, P. J. Hudson, N. Jouanard, K. H. Nguyen, R. S. Ostfeld *et al.*, "Emerging human infectious diseases and the links to global food production," *Nature sustainability*, vol. 2, no. 6, pp. 445–456, 2019.

[26] C. C. McCluskey, "Global stability for an seir epidemiological model with varying infectivity and infinite delay," *Mathematical Biosciences & Engineering*, vol. 6, no. 3, p. 603, 2009.

[27] G. Huang, Y. Takeuchi, W. Ma, and D. Wei, "Global stability for delay sir and seir epidemic models with nonlinear incidence rate," *Bulletin of mathematical biology*, vol. 72, no. 5, pp. 1192–1207, 2010.

[28] L. Gallo, M. Frasca, V. Latora, and G. Russo, "Lack of practical identifiability may hamper reliable predictions in covid-19 epidemic models," *Science advances*, vol. 8, no. 3, p. eabg5234, 2012.

[29] S. Unkel, C. P. Farrington, P. H. Garthwaite, C. Robertson, and N. Andrews, "Statistical methods for the prospective detection of infectious disease outbreaks: a review," *Journal of the Royal Statistical Society: Series A (Statistics in Society)*, vol. 175, no. 1, pp. 49–82, 2012.

[30] C. Farrington, N. J. Andrews, A. Beale, and M. Catchpole, "A statistical algorithm for the early detection of outbreaks of infectious disease," *Journal of the Royal Statistical Society: Series A (Statistics in Society)*, vol. 159, no. 3, pp. 547–563, 1996.

[31] J. Zhang, F.-C. Tsui, M. M. Wagner, and W. R. Hogan, "Detection of outbreaks from time series data using wavelet transform," in *AMIA Annual Symposium Proceedings*, vol. 2003. American Medical Informatics Association, 2003, p. 748.

[32] Y. Le Strat and F. Carrat, "Monitoring epidemiologic surveillance data using hidden markov models," *Statistics in medicine*, vol. 18, no. 24, pp. 3463–3478, 1999.

[33] D. Madigan, "Bayesian data mining for health surveillance," *Spatial and syndromic surveillance for public health*, pp. 203–221, 2005.

[34] Y. Xiao, M. Yang, Z. Zhu, H. Yang, L. Zhang, and S. Ghader, "Modeling indoor-level non-pharmaceutical interventions during the covid-19 pandemic: A pedestrian dynamics-based microscopic simulation approach," *Transport policy*, vol. 109, pp. 12–23, 2021.

[35] Z. Cui, M. Cai, Y. Xiao, Z. Zhu, M. Yang, and G. Chen, "Forecasting the transmission trends of respiratory infectious diseases with an exposure-risk-based model at the microscopic level," *Environmental Research*, vol. 212, p. 113428, 2022.

[36] D. Alvarez Castro and A. Ford, "3d agent-based model of pedestrian movements for simulating covid-19 transmission in university students," *ISPRS International Journal of Geo-Information*, vol. 10, no. 8, p. 509, 2021.

[37] W. O. Kermack and A. G. McKendrick, "A contribution to the mathematical theory of epidemics," *Proceedings of the royal society of london. Series A, Containing papers of a mathematical and physical character*, vol. 115, no. 772, pp. 700–721, 1927.

[38] J. Satsuma, R. Willox, A. Ramani, B. Grammaticos, and A. Carstea, "Extending the sir epidemic model," *Physica A: Statistical Mechanics and its Applications*, vol. 336, no. 3-4, pp. 369–375, 2004.

[39] M. J. Keeling and P. Rohani, *Modeling infectious diseases in humans and animals*. Princeton university press, 2011.

[40] L. Dell'Anna, "Solvable delay model for epidemic spreading: the case of covid-19 in italy," *Scientific Reports*, vol. 10, no. 1, pp. 1–10, 2020.

[41] S. Tiwari, C. Vyasarayani, and A. Chatterjee, "Data suggest covid-19 affected numbers greatly exceeded detected numbers, in four european countries, as per a delayed seiqr model," *Scientific reports*, vol. 11, no. 1, pp. 1–12, 2021.

[42] L. Kleinrock, *Queueing systems: theory*. John Wiley, 1975.

[43] R. G. Gallager, *Discrete stochastic processes*. Springer Science & Business Media, 2012, vol. 321.

[44] A. Papoulis and S. Pillai, "Probability, random variables, and stochastic process, mcgraw-hill, inc," 1991.

[45] J. H. Jones, "Notes on r0," *California: Department of Anthropological Sciences*, vol. 323, pp. 1–19, 2007.

[46] J. Pitman, "Poisson-kingman partitions," *Lecture Notes-Monograph Series*, pp. 1–34, 2003.

[47] E. Dong, H. Du, and L. Gardner, "Covid-19 data repository by the center for systems science and engineering (csse) at johns hopkins university," https://github.com/CSSEGISandData/COVID-19, 2020, accessed: [Access Date].

[48] AP-News, "Germany's covid timeline: from first case to 100,000 dead," https://apnews.com/article/coronavirus-pandemic-health-europe-epidemics-berlin-b61de99739774c1f52b4ba6860054d6d, 2021.

[49] J. Dehning, J. Zierenberg, F. P. Spitzner, M. Wibral, J. P. Neto, M. Wilczek, and V. Priesemann, "Inferring change points in the spread of covid-19 reveals the effectiveness of interventions," *Science*, vol. 369, no. 6500, p. eabb9789, 2020.

[50] S. A. Lauer, K. H. Grantz, Q. Bi, F. K. Jones, Q. Zheng, H. R. Meredith, A. S. Azman, N. G. Reich, and J. Lessler, "The incubation period of coronavirus disease 2019 (covid-19) from publicly reported confirmed cases: estimation and application," *Annals of internal medicine*, vol. 172, no. 9, pp. 577–582, 2020.

[51] H. Bhapkar, P. N. Mahalle, N. Dey, and K. Santosh, "Revisited covid-19 mortality and recovery rates: are we missing recovery time period?" *Journal of Medical Systems*, vol. 44, no. 12, p. 202, 2020.

[52] I. Kiselev, I. Akberdin, and F. Kolpakov, "Delay-differential seir modeling for improved modelling of infection dynamics," *Scientific Reports*, vol. 13, no. 1, p. 13439, 2023.

Narges M.Shahtori (Graduate Student Member, IEEE) received her M.Sc. degree in electrical and computer engineering from Kansas State University (KSU), Manhattan, KS, in 2016. She is currently pursuing her Ph.D. degree with the Electrical and Computer Engineering Department at New York University (NYU). Her research is focused on the intersection of Bayesian modeling and the application of network theory for time-delay systems, particularly in the control of complex time-delay networked nonlinear dynamics.

S. Farokh Atashzar (Senior Member, IEEE) is currently an assistant professor at New York University (NYU), New York, NY, USA, and has been jointly appointed with the Department of Electrical and Computer Engineering and the Department of Mechanical and Aerospace Engineering. He is also affiliated with the Department of Biomedical Engineering, NYU, NYU WIRELESS, and NYU Center for Urban Science and Progress. Before joining NYU, he was a postdoctoral scientist at Imperial College in London, London, U.K. At NYU, he is the Director of the Medical Robotics and Interactive Intelligent Technologies (MERIIT) Laboratory. The Laboratory is mainly funded by the U.S. National Science Foundation. Prof. Atashzar was a recipient of several awards, including the 2021 Outstanding Associate Editor of IEEE Robotics and Robotics. He is currently an Associate Editor for IEEE Transactions on Robotics and IEEE Transactions on Haptics.